



## Theoretical Investigations of State Specific Hydrogen Atom Transfer in 8-Formyl-7-hydroxy-4-methylcoumarin

K. JAGADEESHA<sup>1,\*</sup>, Y.L. RAMU<sup>1</sup>, T. SHIVALINGASWAMY<sup>1</sup> and M. RAMEGOWDA<sup>2</sup>

<sup>1</sup>P.G. Department of Physics, Government College (Autonomous), Mandya-571401, India

<sup>2</sup>Department of Physics, Mandya University, Mandya-571401, India

\*Corresponding author: E-mail: ashajaga.2008@gmail.com

Received: 7 August 2021;

Accepted: 21 September 2021;

Published online: 11 January 2022;

AJC-20645

Excited state intramolecular hydrogen transfer (ESIHT) reaction of 8-formyl-7-hydroxy-4-methyl coumarin (FC) in its pure and hydrated state FC-(H<sub>2</sub>O)<sub>4</sub> (FCH) has been studied by implementing state specific time dependent density functional theory (SS-TDDFT) along with the effective fragment potential (EFP1) method for solvation with discrete water molecules. The intramolecular hydrogen bond formed between hydroxyl hydrogen (H18) and formyl oxygen (O15) and intermolecular hydrogen bonds formed due to microsolvation were explored. The studies of electrostatic potential, natural charge analysis, difference electron density map and UV-Vis spectra of both FC and FCH molecules establish the intramolecular charge transfer (ICT) states of the molecules. The vertical excitation from S<sub>0</sub> to S<sub>1</sub> state causes the transfer of hydroxyl hydrogen to formyl oxygen and from S<sub>1</sub> to S<sub>3</sub> causes the transfer of the hydrogen atom back to hydroxyl oxygen. Potential energy surface scans along intramolecular hydrogen bonding at the ground and excited states confirm the state specific ESIHT reaction in both FC and FCH molecules.

**Keywords:** Coumarin, Intramolecular hydrogen transfer, Intramolecular charge transfer, Effective fragment potential.

### INTRODUCTION

The quantum theory of atom in molecules (QTAIM) has been useful to characterize both the intramolecular and intermolecular interaction in hydrogen bonding complexes at the ground and excited states [1,2]. The intermolecular hydrogen bonding is a site specific solute-solvent interaction which plays an immensely important role on the spectra of biologically active molecules. Theoretical study of the hydrogen bonds is much necessary for understanding the photo-physical properties of some electron donor and acceptor natured organic molecules at both ground and excited states [3-8]. Effective fragment potential (EFP) method is computationally inexpensive way of modeling intermolecular interactions in non-covalently bonded systems. The DFT based EFP (EFP1/DFT) method was used in the study of microsolvation effects of organic and biological molecules. Effective fragment potential (EFP1) was established explicitly for solvation with several numbers of water molecules and is interfaced with the polarizable continuum model (PCM) [9-11]. Time dependent density functional theory

(TDDFT) computations have been used in understanding the structural, molecular, electronic and photo-physical properties of many molecules in the ground and excited states [12-14]. In most of the organic and biological molecules, there will be an intramolecular hydrogen atom transfer/proton transfer (ESIHT/ESIPT) [15-18] at the excited state due to photo-induction. At the excited state, reshuffling of atoms takes place within the molecule along with hydrogen transfer, which has been extensively examined in the photo-induced reactions. The alteration of hydrogen bond morphology due to microsolvation causes to inspire ESIPT/ESIHT process in some organic and biological molecules [19-23].

Hydroxycoumarins belong to the electron donor-acceptor aromatic compounds as they contain a donor hydroxyl group and an acceptor carbonyl group attached to a different aromatic ring finding applications in various fields [24]. 7-Hydroxycoumarins and their derivatives were widely explored for their biological activities such as antimutagenic [25], fluorogenic enzyme substrates [26] and antifungals [27]. These compounds can also be used as colourants, laser dyes and fluorophores/

chromophores [28,29]. The charge transfer character associated with ESIPT/ESIHT is correlated to the photophysical features of these molecules [20,21,30]. 8-Formyl-7-hydroxy-4-methyl coumarin (FC) molecule is one of the interesting derivatives of 7-hydroxycoumarin mainly used in the synthesis of Schiff bases and scaffolds [31,32]. It can form an intramolecular hydrogen bonding between hydroxyl group and formyl group and can also form four intermolecular hydrogen bonds with solvent molecules by carbonyl and hydroxyl groups. In the present study, the electronic structure and intramolecular charge transfer (ICT) states of 8-formyl-7-hydroxy-4-methyl coumarin (FC) and FC-(H<sub>2</sub>O)<sub>4</sub> (FCH) molecules along with the excited state intramolecular hydrogen transfer (ESIHT) process have been investigated.

### COMPUTATIONAL METHODS

Natural bond orbital (NBO) [33] integrated GAMESS [34,35] software suite is implemented to explore the electronic structure of the 8-formyl-7-hydroxy-4-methyl coumarin (FC) and FC-(H<sub>2</sub>O)<sub>4</sub> (FCH) molecules at ground (S<sub>0</sub>), first excited (S<sub>1</sub>) and third excited (S<sub>3</sub>) states at the level of DFT [36-40] and state specific time dependent density functional theory (SS-TDDFT) [41,42] with B3LYP [43,44] functional and cc-pVDZ basis set [45]. FCH complex is composed by adding explicit water molecules to FC using EFP1 method. UV-Vis

absorption spectra of FC and FCH have been simulated by applying SS-TDDFT/cc-pVDZ/B3LYP/PCM/EFP1 [46-48]. The ICT states of both molecules were carried out by computing molecular orbital's, difference density map, electrostatic potential and natural charges on various atoms and groups at S<sub>0</sub>, S<sub>1</sub> and S<sub>3</sub> states. In both FC and FCH molecules, an intramolecular hydrogen atom transfer can be observed with the transfer of the hydroxyl hydrogen to formyl oxygen at S<sub>1</sub> state and the back transfer is observed at S<sub>3</sub> state. In order to confirm the ESIHT process potential energy scan along the hydrogen bondings O14-H18...O15=C11/C3=O14 H18-O15 has been performed at the level of DFT/cc-pVDZ/B3LYP/SS-TDDFT in S<sub>0</sub>, S<sub>1</sub> and S<sub>3</sub> states.

### RESULTS AND DISCUSSION

**Structural properties at ground state:** 8-Formyl-7-hydroxy-4-methyl coumarin (FC) and FC-(H<sub>2</sub>O)<sub>4</sub> (FCH) molecules were optimized at the level DFT/B3LYP/cc-pVDZ along with the computations of electrostatic potential, molecular orbitals, difference electron density map and natural charges. The respective ground state molecular structures and plots of electrostatic potential and difference electron density map are depicted in Fig. 1. The optimized parameters like bond lengths and bond angles are given in Tables 1 and 2. In both molecules, benzene and pyrone rings lie in a plane. Interestingly, it

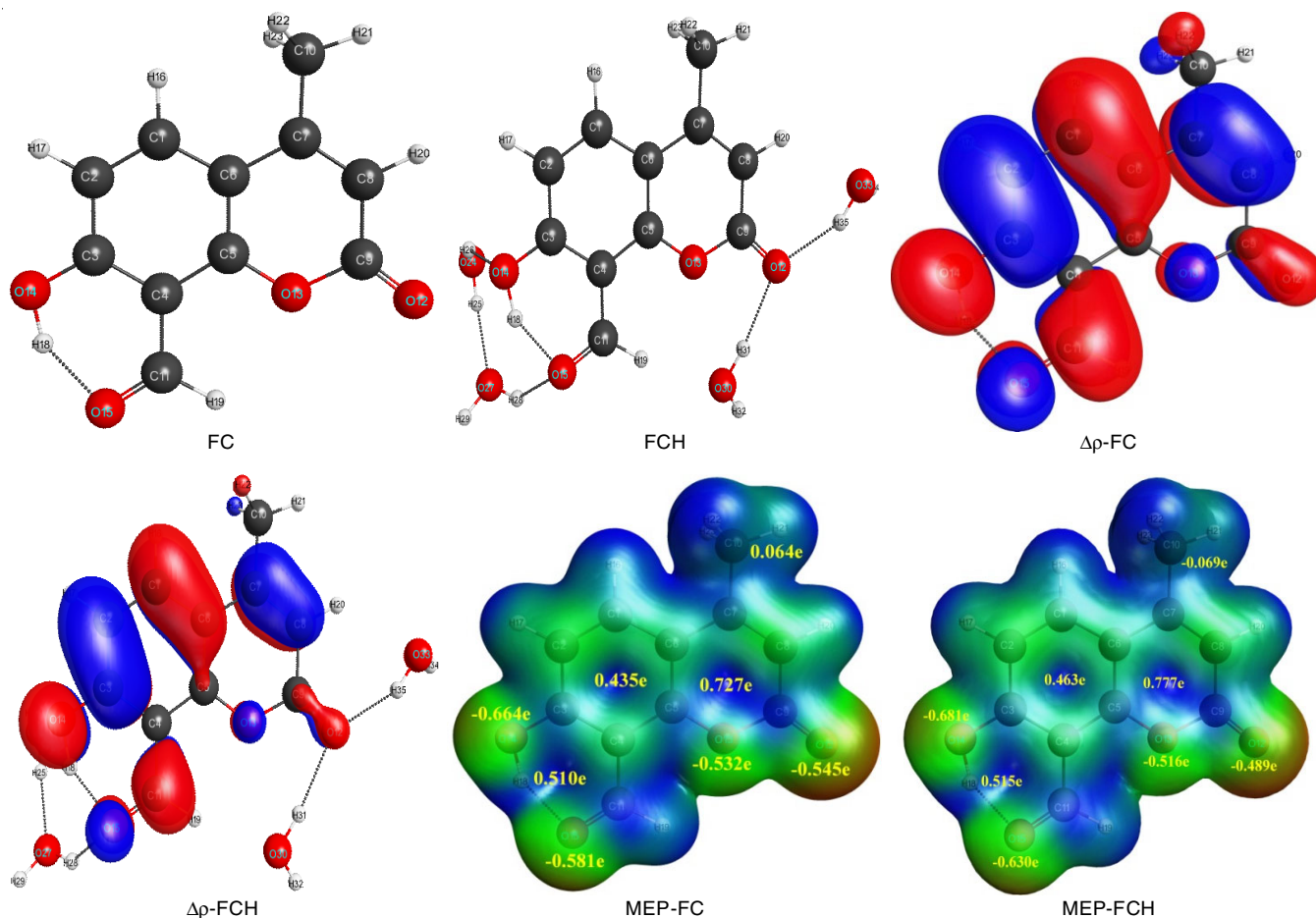


Fig. 1. Optimized molecular structures, difference electron density map and MEP along with natural charges on various groups and atoms of FC and FCH molecules at S<sub>0</sub> state

Bond lengths (Å)	FC			FCH		
	$S_0$	$S_1$	$S_3$	$S_0$	$S_1$	$S_3$
R(1-2)	1.383	1.391	1.385	1.382	1.391	1.382
R(1-6)	1.417	1.405	1.417	1.419	1.405	1.420
R(1-16)	1.091	1.090	1.084	1.091	1.090	1.091
R(2-3)	1.411	1.449	1.420	1.412	1.447	1.430
R(2-17)	1.090	1.092	1.084	1.091	1.092	1.091
R(3-4)	1.424	1.446	1.424	1.421	1.442	1.432
R(3-14)	1.330	1.269	1.327	1.333	1.274	1.313
R(4-5)	1.417	1.393	1.411	1.414	1.391	1.409
R(4-11)	1.458	1.442	1.448	1.460	1.443	1.466
R(5-6)	1.407	1.475	1.446	1.405	1.471	1.436
R(5-13)	1.354	1.347	1.347	1.354	1.347	1.359
R(6-7)	1.453	1.422	1.438	1.452	1.424	1.451
R(7-8)	1.362	1.381	1.406	1.367	1.384	1.409
R(7-10)	1.505	1.506	1.498	1.504	1.505	1.496
R(8-9)	1.451	1.442	1.419	1.444	1.439	1.421
R(8-20)	1.091	1.090	1.084	1.090	1.089	1.092
R(9-12)	1.204	1.208	1.216	1.220	1.221	1.233
R(9-13)	1.416	1.411	1.464	1.391	1.392	1.428
R(10-21)	1.098	1.098	1.093	1.098	1.098	1.100
R(10-22)	1.103	1.102	1.100	1.103	1.102	1.108
R(10-23)	1.103	1.102	1.101	1.103	1.102	1.108
R(11-15)	1.237	1.323	1.250	1.242	1.331	1.239
R(11-19)	1.108	1.090	1.099	1.105	1.090	1.106
R(14-18)	1.002	1.566	1.006	1.004	1.547	0.997
R(15-18)	1.650	1.028	1.624	1.642	1.032	1.878

Bond angles (°)	FC			FCH		
	$S_0$	$S_1$	$S_3$	$S_0$	$S_1$	$S_3$
A(2-1-6)	122.4	120.5	122.5	122.2	120.3	122.3
A(2-1-16)	118.7	119.7	118.9	118.8	119.8	119.1
A(1-2-3)	119.8	123.0	120.0	119.9	123.0	120.5
A(1-2-17)	121.7	121.0	121.8	121.6	120.9	121.9
A(6-1-16)	118.9	119.8	118.5	119.0	119.9	118.7
A(1-6-5)	117.4	117.1	116.9	117.1	116.9	116.7
A(1-6-7)	124.4	124.4	123.7	124.9	124.8	123.5
A(3-2-17)	118.5	116.0	118.2	118.5	116.1	117.6
A(2-3-4)	119.8	117.7	120.0	120.0	118.1	119.4
A(2-3-14)	119.0	121.0	118.5	119.0	120.9	116.3
A(4-3-14)	121.2	121.3	121.4	121.0	121.0	124.2
A(3-4-5)	118.7	118.4	119.0	118.2	117.9	118.4
A(3-4-11)	119.4	119.3	118.9	120.2	120.1	120.8
A(3-14-18)	106.3	100.8	106.8	106.0	100.5	114.3
A(5-4-11)	121.9	122.3	122.1	121.6	122.0	120.8
A(4-5-6)	121.8	123.3	121.5	122.6	123.9	122.7
A(4-5-13)	116.4	116.7	116.3	116.1	116.4	115.1
A(4-11-15)	122.9	120.9	122.6	121.6	119.6	121.7
A(4-11-19)	117.1	122.8	117.6	118.1	123.3	117.1
A(6-5-13)	121.8	120.0	122.2	121.3	119.7	122.3
A(5-6-7)	118.2	118.5	119.4	118.0	118.4	119.8
A(5-13-9)	122.6	122.9	120.3	122.9	123.0	119.8
A(6-7-8)	118.8	119.0	116.7	119.2	119.3	115.7
A(6-7-10)	120.2	120.8	121.5	120.1	120.8	121.8
A(8-7-10)	121.0	120.2	121.8	120.7	119.8	122.5
A(7-8-9)	123.1	122.8	124.5	121.9	121.7	124.1
A(8-9-12)	127.7	127.0	130.0	128.0	127.4	129.4
A(8-9-13)	115.5	116.8	116.4	116.7	117.9	118.1
A(12-9-13)	116.8	116.2	113.5	115.3	114.7	112.5
A(15-11-19)	120.0	116.3	119.7	120.3	117.0	121.2
A(11-15-18)	100.4	104.5	101.1	101.2	104.4	104.5
A(14-18-15)	149.8	153.2	149.1	150.0	154.2	134.2

is observed that an intramolecular hydrogen bonding exists between hydroxyl hydrogen and formyl oxygen. The formation of intramolecular hydrogen bonding, O14-H18...O15=C11 makes the hydroxyl and formyl groups also lie in the same plane. The hydration to the FC molecule does not deviate the structural parameters including the natural charges, except the parameters associated with the hydroxyl, carbonyl and formyl groups, which were altered slightly due to the formation of intermolecular hydrogen bonds. In the difference charge density graph, electron diminution fields ( $\rho^+$ ) were established on C2, C3, C7, C8, O13 and O15 atoms, whereas the electron accretion fields ( $\rho^-$ ) were localized on C1, C6, C11, C9, O12 and O14 atoms, respectively. The electrostatic potential map along with the natural charges on various groups and atoms signaling that the hydroxyl and carbonyl groups were more reactive for electrophiles. The plot of molecular orbital's and difference electron density map indicate that the electronic charge concentrated on the hydroxyl, carbonyl and formyl oxygen and also on the central part of the two rings.

**ICT states of the molecules:** In order to identify the ICT states of the molecules, UV-Vis absorption spectra of FC and FCH molecules have been simulated in the gas phase, water and chloroform solvents using SS-TDDFT/cc-pVDZ/B3LYP/PCM/EFP1 method. The vertical absorption energies, oscillator strengths and probable wave functions are presented in Table-3, and the spectra are displayed in Fig. 2. On observing the corresponding oscillator strengths,  $S_1$  and  $S_3$  states were found to be more probable in gas and solvent phase to study ICT states of

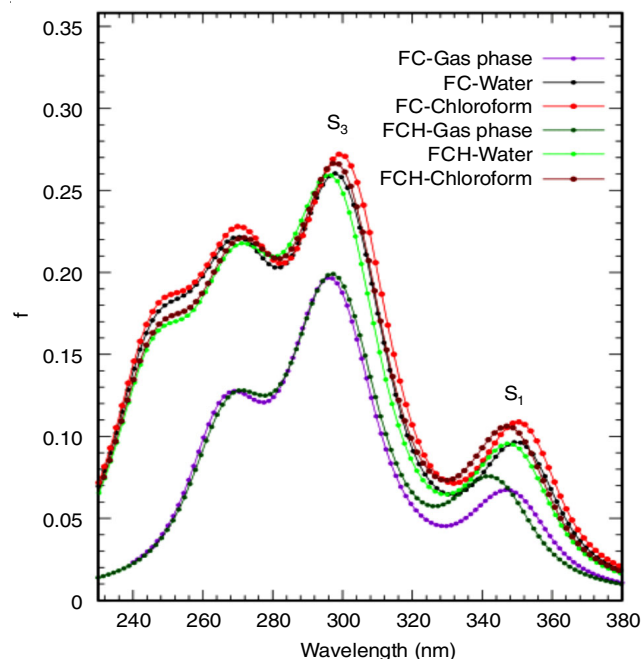


Fig. 2. Theoretical simulated absorption spectra of FC and FCH molecules in gas phase, water and chloroform solvents

TABLE-3  
ABSORPTION WAVELENGTH [ $\lambda_a$  (nm)] AND OSCILLATOR STRENGTH (f)  
OF FC AND FCH MOLECULES WITH PROBABLE TRANSITIONS

Molecule	State	TDDFT/B3LYP/cc-pVDZ						Expt. [Ref. 49]
		Gas phase		Water		Chloroform		
		$\lambda_a$	f	$\lambda_a$	f	$\lambda_a$	f	
FC	S <sub>1</sub>	349	0.067	350	0.095	350	0.106	350
		H→L (0.916)		H→L (0.941)		H→L (0.943)		
		H→L+1 (0.332)		H→L+1 (0.268)		H→L+1 (0.263)		
FC	S <sub>3</sub>	296	0.223	299	0.292	300	0.304	304
		H→L (0.335)		H→L (0.275)		H→L (0.270)		
		H→L+1 (0.919)		H→L+1 (-0.945)		H→L+1 (0.948)		
FCH	S <sub>1</sub>	344	0.072	348	0.094	347	0.106	
		H→L (0.903)		H→L (0.937)		H→L (-0.937)		
		H→L+1 (0.360)		H→L+1 (-0.279)		H→L+1 (-0.280)		
FCH	S <sub>3</sub>	297	0.228	297	0.282	299	0.292	
		H→L (-0.372)		H→L (-0.290)		H→L (-0.291)		
		H→L+1 (0.900)		H→L+1 (-0.936)		H→L+1 (-0.938)		

both FC and FCH molecules. The computed absorption wavelengths in chloroform are in good agreement with the experimental values [49]. The blue shifts of 1-3 nm in microsolvated molecule indicate the strengthening of hydrogen bondings in the excited states.

Using ground state coordinates, FC and FCH molecules were optimized at S<sub>1</sub> and S<sub>3</sub> states and also using the S<sub>1</sub> state optimized coordinates both molecules were optimized at S<sub>3</sub> state. In S<sub>1</sub> and S<sub>3</sub> states the geometrical parameters associated with the pyrone ring, hydroxyl, carbonyl and formyl groups were slightly altered. The intermolecular hydrogen bondings slightly get disturbed in S<sub>3</sub> state as compared to S<sub>1</sub> state. In S<sub>1</sub> state of both molecules the hydrogen atom H18 transferred from the hydroxyl group to formyl group, whereas in S<sub>3</sub> state no transfer of hydrogen atom is observed. The optimization of the S<sub>3</sub> state of molecules using S<sub>1</sub> state coordinates brings back the hydrogen atom H18 from formyl group to hydroxyl group. The excited state molecular diagrams along with the molecular electrostatic potential maps are shown in Fig. 3 and natural charges are listed in Table-4.

In S<sub>1</sub> and S<sub>3</sub> states, the positive charge on benzene and pyrone rings increases in both FC and FCH molecules. In FC molecule negative charge on hydroxyl oxygen O14 decreases at S<sub>1</sub> and S<sub>3</sub> states, where as in FCH molecule charge on O14 at S<sub>1</sub> state remains same as S<sub>0</sub> state and decreases in S<sub>3</sub> state. In both FC and FCH molecules, the negative charge on formyl oxygen O15 increases at S<sub>1</sub> state and decreases at S<sub>3</sub> state. On observing overall change in the natural charges of the hydroxyl (-O14H18) and formyl (-C11O15H19) groups of both FC and FCH molecules, negative charge on the formyl group appreciably increases only in the S<sub>1</sub> state. So hydrogen transfer can be observed only in the S<sub>1</sub> state.

**ESIHT process:** In order to establish the intramolecular hydrogen atom transfer from the hydroxyl group to formyl group at S<sub>1</sub> and S<sub>3</sub> states, potential energy scan along the hydrogen atom transferred paths O14-H18...O15=C11 and C3=O14...H18-O15 have been performed at the level of DFT/SS-TDDFT/cc-pVDZ/B3LYP/EFP1 for both FC and FCH mole-

TABLE-4  
NATURAL CHARGES ON VARIOUS ATOMS AND GROUPS  
OF FC AND FCH MOLECULES AT S<sub>0</sub>, S<sub>1</sub> AND S<sub>3</sub> STATES

Atom	FC			FCH		
	S <sub>0</sub>	S <sub>1</sub>	S <sub>3</sub>	S <sub>0</sub>	S <sub>1</sub>	S <sub>3</sub>
C1	-0.154	-0.227	-0.206	-0.147	-0.221	-0.186
C2	-0.291	-0.190	-0.242	-0.283	-0.176	-0.234
C3	0.426	0.420	0.417	0.428	0.424	0.438
C4	-0.286	-0.304	-0.284	-0.278	-0.297	-0.239
C5	0.426	0.469	0.396	0.421	0.471	0.355
C6	-0.175	-0.111	-0.057	-0.171	-0.106	-0.040
C7	0.047	0.040	-0.047	0.058	0.047	-0.064
C8	-0.350	-0.314	-0.362	-0.355	-0.314	-0.335
C9	0.779	0.766	0.710	0.788	0.776	0.710
C10	-0.667	-0.668	-0.709	-0.670	-0.670	-0.670
C11	0.402	0.209	0.336	0.407	0.206	0.358
O12	-0.545	-0.489	-0.524	-0.645	-0.581	-0.643
O13	-0.532	-0.509	-0.520	-0.516	-0.499	-0.539
O14	-0.664	-0.652	-0.636	-0.681	-0.681	-0.606
O15	-0.581	-0.640	-0.548	-0.630	-0.682	-0.609
H16	0.240	0.240	0.258	0.242	0.247	0.247
H17	0.250	0.245	0.265	0.251	0.247	0.250
H18	0.510	0.508	0.526	0.515	0.510	0.600
H19	0.184	0.207	0.224	0.241	0.254	0.237
H20	0.251	0.256	0.261	0.285	0.298	0.270
H21	0.244	0.244	0.255	0.248	0.248	0.246
H22	0.243	0.250	0.244	0.245	0.251	0.228
H23	0.244	0.250	0.243	0.246	0.251	0.227
O14 + H18	-0.154	-0.144	-0.110	-0.166	-0.171	-0.006
C11 + O15 + H19	0.005	-0.225	0.012	0.018	-0.223	-0.015

cules. The plots are depicted in Figs. 4 and 5. On observation of Fig. 4, it is noticed that FC and FCH molecules get excited to unrelaxed S<sub>1</sub><sup>\*</sup> state by absorbing the radiations of energy 3.55 eV and 3.60 eV, respectively, the OH bond gets elongated to 1.72 Å and 1.76 Å. At this point, the hydrogen atom is transferred from the hydroxyl group to formyl group and the molecules get relaxed in the S<sub>1</sub> state. On further excitation of the molecules from S<sub>1</sub> to S<sub>3</sub><sup>\*</sup> state by irradiating the radiations of energy 1.41 eV and 2.73 eV, the -OH bond of FC and FCH

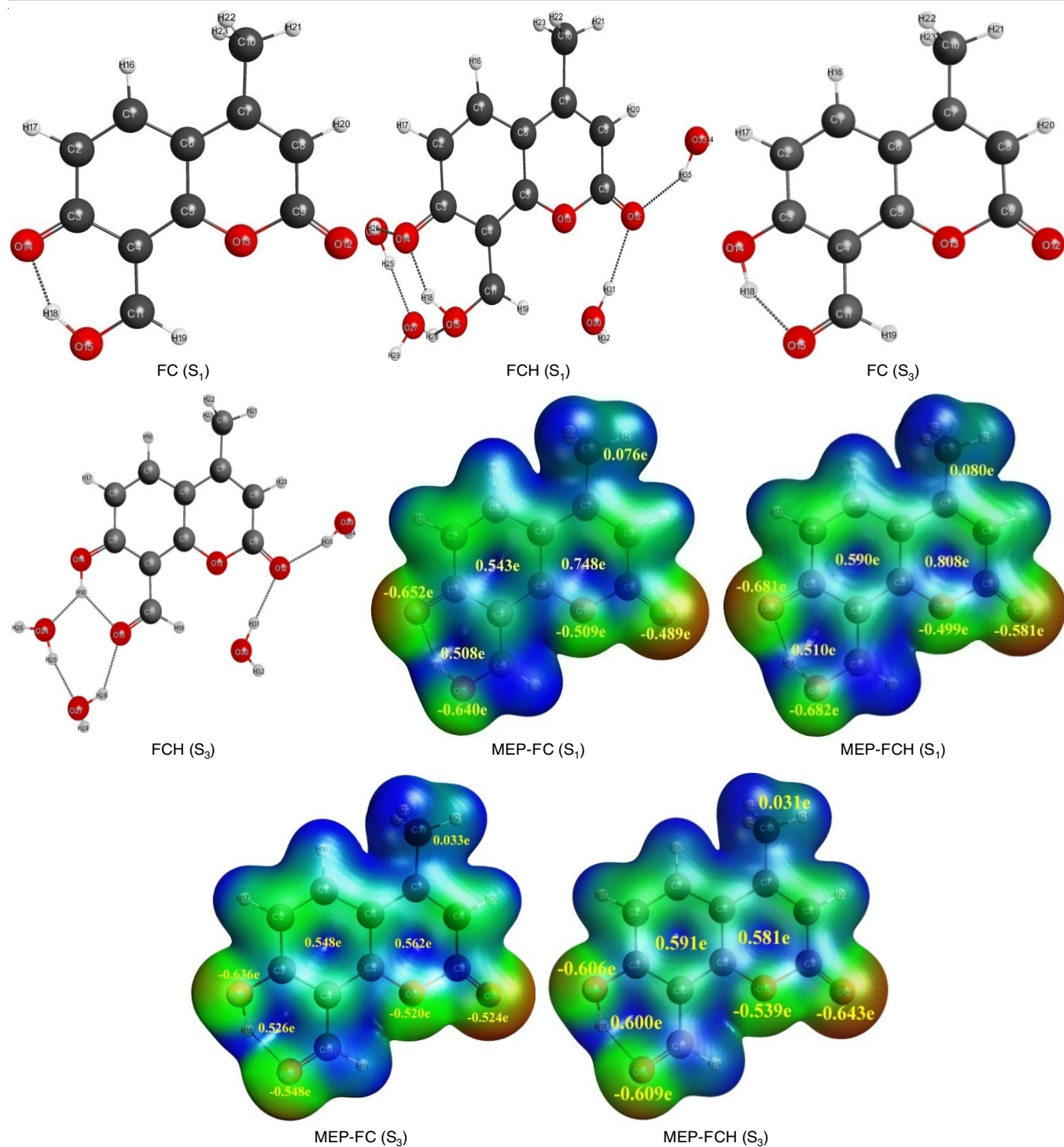


Fig. 3. Optimized molecular structures and MEP along with natural charges on various groups and atoms of FC and FCH molecules at  $S_1$  and  $S_3$  state

get contracted to 1.44 Å and 1.24 Å, respectively and the hydrogen atom get transferred back from formyl group to the hydroxyl group. The downward transition from  $S_1$  to unrelaxed ground state,  $S_0^*$  also contracts the intramolecular hydrogen bondings to 1.36 Å and 1.35 Å, respectively in FC and FCH molecules and brings back the H18 atom from formyl to hydroxyl group and the molecule exist in the  $S_0$  state. As shown in Fig. 5, the direct excitation of the molecules from  $S_0$  to  $S_3$  state, the truancy of hydrogen atom transfer can be observed.

This confirms the state specific hydrogen atom transfer in FC and FCH molecules.

### Conclusion

Electronic structure properties of 8-formyl-7-hydroxy-4-methyl coumarin (FC) manifest the existence of the intramolecular hydrogen bonding in its pure and hydrated states. The hydration of the molecule using EFP1 method indicates the possibility of four intermolecular hydrogen bonding sites. The

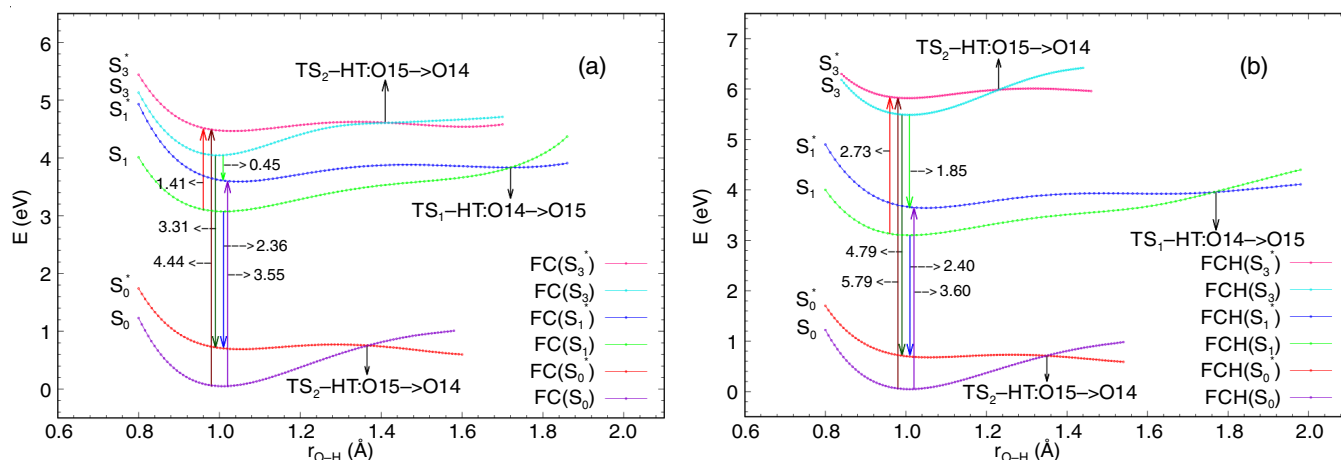


Fig. 4. Potential energy plots along the hydrogen atom transfer path of (a) FC and (b) FCH molecules

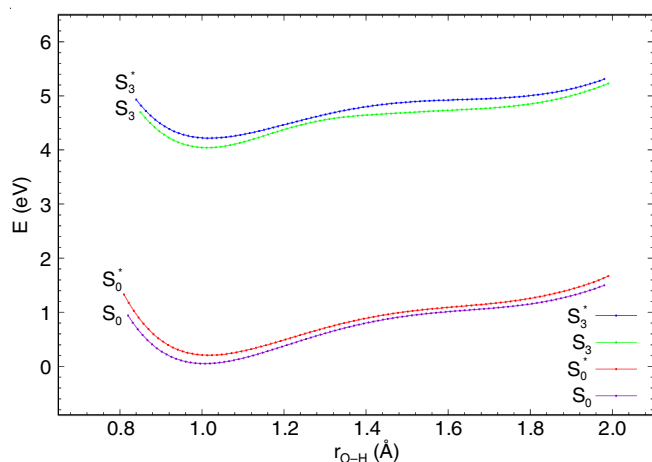


Fig. 5. Potential energy plots of the molecules on direct excitation from  $S_0$  to  $S_3$  state

electrostatic potential plot, natural charge analysis, difference electron density map and UV-Vis spectra of both FC and FCH molecules emphasize the study of ICT states of the molecules. In addition to these, the potential energy surface scan establishes the intramolecular hydrogen atom transfer from the hydroxyl group to formyl group on excitation of the molecules from ground state to first excited state. On further excitation from first to third excited state hydrogen gets transferred back from formyl to the hydroxyl group. Also potential energy plots confirmed the truancy of hydrogen atom transfer on direct excitation from ground to third excited state. This state specific ESIHT study contributes to the ongoing research on the biological and chemical activity of the derivatives of coumarin molecule.

#### CONFLICT OF INTEREST

The authors declare that there is no conflict of interests regarding the publication of this article.

#### REFERENCES

- P.S.V. Kumar, V. Raghavendra and V. Subramanian, *J. Chem. Sci.*, **128**, 1527 (2016); <https://doi.org/10.1007/s12039-016-1172-3>
- F. Fuster and S.J. Grabowski, *J. Phys. Chem. A*, **115**, 10078 (2011); <https://doi.org/10.1021/jp2056859>
- D.K. Palit, T. Zhang, S. Kumazaki and K. Yoshihara, *J. Phys. Chem. A*, **107**, 10798 (2003); <https://doi.org/10.1021/jp030633a>
- Y. Liu, J. Ding, R. Liu, D. Shi and J. Sun, *J. Photochem. Photobiol. Chem.*, **201**, 203 (2009); <https://doi.org/10.1016/j.jphotochem.2008.10.016>
- M. Miao and Y. Shi, *J. Comput. Chem.*, **32**, 3058 (2011); <https://doi.org/10.1002/jcc.21888>
- M. Zhang, B. Ren, Y. Wang and C. Zhao, *Spectrochim. Acta A Mol. Biomol. Spectrosc.*, **101**, 191 (2013); <https://doi.org/10.1016/j.saa.2012.09.045>
- M. Ramegowda, *New J. Chem.*, **37**, 2648 (2013); <https://doi.org/10.1039/c3nj00446e>
- M. Ramegowda, *Spectrochim. Acta A Mol. Biomol. Spectrosc.*, **137**, 99 (2015); <https://doi.org/10.1016/j.saa.2014.08.017>
- M.S. Gordon, M.A. Freitag, P. Bandyopadhyay, J.H. Jensen, V. Kairys and W.J. Stevens, *J. Phys. Chem. A*, **105**, 293 (2001); <https://doi.org/10.1021/jp002747h>
- M.S. Gordon, M.A. Freitag, P. Bandyopadhyay, J.H. Jensen, V. Kairys and W.J. Stevens, *J. Phys. Chem. A*, **105**, 293 (2001); <https://doi.org/10.1021/jp002747h>
- I. Adamovic, M.A. Freitag and M.S. Gordon, *J. Chem. Phys.*, **2003**, 6725 (2015); <https://doi.org/10.1063/1.1559912>
- P. Arora, L.V. Slipchenko, S.P. Webb, A. DeFusco and M.S. Gordon, *J. Phys. Chem. A*, **114**, 6742 (2010); <https://doi.org/10.1021/jp101780r>
- N. De Silva and F. Zahariev, *J. Chem. Phys.*, **134**, 54111 (2011); <https://doi.org/10.1063/1.3523578>
- S. Yoo, F. Zahariev, S. Sok and M.S. Gordon, *J. Chem. Phys.*, **129**, 144112 (2008); <https://doi.org/10.1063/1.2992049>
- A. Douhal, S.K. Kim and A.H. Zewail, *Nature*, **378**, 260 (1995); <https://doi.org/10.1038/378260a0>
- D.S. Lu and G.A. Voth, *J. Am. Chem. Soc.*, **120**, 4006 (1998); <https://doi.org/10.1021/ja973397o>
- D. Marx, M.E. Tuckerman, J. Hutter and M. Parrinello, *Nature*, **397**, 601 (1999); <https://doi.org/10.1038/17579>
- M.-W. Chung, T.-Y. Lin, C.-C. Hsieh, K.-C. Tang, H. Fu, P.-T. Chou, S.-H. Yang and Y. Chi, *J. Phys. Chem. A*, **114**, 7886 (2010); <https://doi.org/10.1021/jp1036102>
- A. Kyrychenko and J. Waluk, *J. Phys. Chem. A*, **110**, 11958 (2006); <https://doi.org/10.1021/jp063426u>
- M. Ramegowda, K.N. Ranjitha and T.N. Deepika, *New J. Chem.*, **40**, 2211 (2016); <https://doi.org/10.1039/C5NJ02917A>

21. K. Jagadeesha, Y.L. Ramu, M. Ramegowda and N.K. Lokanath, *Spectrochim. Acta A Mol. Biomol. Spectrosc.*, **208**, 325 (2019); <https://doi.org/10.1016/j.saa.2018.10.015>
22. Y.L. Ramu, K. Jagadeesha, T. Shivalingaswamy and M. Ramegowda, *Chem. Phys. Lett.*, **739**, 137030 (2020); <https://doi.org/10.1016/j.cplett.2019.137030>
23. K.L. Han and G.J. Zhao, *The Experimental and Theoretical Study on ESIHT/ESIPT along with the Excited State Intra/Intermolecular HB Dynamics of Many Organic and Biomolecules via Microsolvation*, John Wiley & Sons Ltd.; New York (2011).
24. L.D. Lavis and R.T. Raines, *ACS Chem. Biol.*, **3**, 142 (2008); <https://doi.org/10.1021/cb700248m>
25. S.P. Pillai, S.R. Menon, L.A. Mitscher, C.A. Pillai and D.M. Shankel, *J. Nat. Prod.*, **62**, 1358 (1999); <https://doi.org/10.1021/np990048u>
26. H. Khalfan, R. Abuknesha, M. Rand-Weaver, R.G. Price and D. Robinson, *Histochem. J.*, **18**, 497 (1986); <https://doi.org/10.1007/BF01675617>
27. S. Sardari, Y. Mori, K. Horita, R.G. Micetich, S. Nishibe and M. Daneshlab, *Bioorg. Med. Chem.*, **7**, 1933 (1999); [https://doi.org/10.1016/S0968-0896\(99\)00138-8](https://doi.org/10.1016/S0968-0896(99)00138-8)
28. D.E. Polyansky and D.C. Neckers, *J. Phys. Chem. A*, **109**, 2793 (2005); <https://doi.org/10.1021/jp044554q>
29. S.Y. Park, Y. Kubota, K. Funabiki and M. Matsui, *Chem. Lett.*, **38**, 162 (2009); <https://doi.org/10.1246/cl.2009.162>
30. M. Savarese, P.A. Netti, C. Adamo, N. Rega and I. Ciofini, *J. Phys. Chem. B*, **117**, 16165 (2013); <https://doi.org/10.1021/jp406301p>
31. M.B. Halli, R.B. Sumathi and M. Kinni, *Spectrochim. Acta A Mol. Biomol. Spectrosc.*, **99**, 46 (2012); <https://doi.org/10.1016/j.saa.2012.08.089>
32. A. Al-Kawkabani, B. Boutemour-Kheddis, M. Makhloufi-Chebli, M. Hamdi, O. Talhi and A.M.S. Silva, *Tetrahedron Lett.*, **54**, 5111 (2013); <https://doi.org/10.1016/j.tetlet.2013.07.047>
33. E.D. Glendenning, J.K. Badenhop, A.E. Reed, J.E. Carpenter, J.A. Bohmann, C.M. Morales, C.R. Landis and F. Weinhold, *Theoretical Chemistry Institute, University of Wisconsin, Madison, WI, USA* (2013).
34. M.W. Schmidt, K.K. Baldrige, J.A. Boatz, S.T. Elbert, M.S. Gordon, J.H. Jensen, S. Koseki, N. Matsunaga, K.A. Nguyen, S.J. Su, T.L. Windus, M. Dupuis and J.A. Montgomery, *J. Comput. Chem.*, **14**, 1347 (1993); <https://doi.org/10.1002/jcc.540141112>
35. M.S. Gordon and M.W. Schmidt, Eds.: C.E. Dykstra, G. Frenking, K.S. Kim and G.E. Scuseria, *Advances in Electronic Structure Theory: GAMESS a Decade Later*; In: *Theory and Applications of Computational Chemistry*, Elsevier, pp. 1167-1189 (2005).
36. R.G. Parr and W. Yang, *Density-Functional Theory of Atoms, Molecules*, Oxford University Press: New York (1989).
37. K. Kim and K.D. Jordan, *J. Phys. Chem.*, **98**, 10089 (1994); <https://doi.org/10.1021/j100091a024>
38. P.J. Stephens, F.J. Devlin, C.F. Chabalowski and M.J. Frisch, *J. Phys. Chem.*, **98**, 11623 (1994); <https://doi.org/10.1021/j100096a001>
39. T.R. Cundari and W.J. Stevens, *J. Chem. Phys.*, **98**, 5555 (1993); <https://doi.org/10.1063/1.464902>
40. P.J. Hay and W.R. Wadt, *J. Chem. Phys.*, **82**, 270 (1985); <https://doi.org/10.1063/1.448799>
41. S. Tokura, T. Sato, T. Tsuneda, T. Nakajima and K. Hirao, *J. Comput. Chem.*, **29**, 1187 (2008); <https://doi.org/10.1002/jcc.20871>
42. M. Chiba, T. Tsuneda and K. Hirao, *Chem. Phys. Lett.*, **420**, 391 (2006); <https://doi.org/10.1016/j.cplett.2006.01.015>
43. A.D. Becke, *J. Chem. Phys.*, **98**, 5648 (1993); <https://doi.org/10.1063/1.464913>
44. A.D. Becke, *Phys. Rev. A*, **38**, 3098 (1988); <https://doi.org/10.1103/PhysRevA.38.3098>
45. T.H. Dunning Jr., *J. Chem. Phys.*, **90**, 1007 (1989); <https://doi.org/10.1063/1.456153>
46. F. Furche and R. Ahlrichs, *J. Chem. Phys.*, **121**, 12772 (2004); <https://doi.org/10.1063/1.1824903>
47. H. Li, C.S. Pomelli and J.H. Jensen, *Theor. Chim. Acta*, **109**, 71 (2003); <https://doi.org/10.1007/s00214-002-0427-x>
48. J. Perdew, M. Ernzerhof and K. Burke, *J. Chem. Phys.*, **105**, 9982 (1996); <https://doi.org/10.1063/1.472933>
49. H. Moghania, A. Mobinikhaledi and R. Monjezi, *J. Mol. Struct.*, **1052**, 135 (2013); <https://doi.org/10.1016/j.molstruc.2013.08.043>